

Research Methods on the Influence of Characteristics of Asperity

Di Wu

Key Laboratory of Earthquake Engineering and Applied Technique of Guangdong Province
Guangzhou University Guangzhou, China
Research Institute of Structure Engineer and Disaster Reduction
Tongji University Shanghai, China
State Key Laboratory of Subtropical Building Science
South China University of Technology Guangzhou, China

Luo Qifeng

Research Institute of Structure Engineer and Disaster
Reduction Tongji University
Shanghai, China
State Key Laboratory of Subtropical Building Science
South China University of Technology
Guangzhou, China

Jie Cui

Key Laboratory of Earthquake Engineering and Applied
Technique of Guangdong Province
Guangzhou University
Guangzhou, China

Abstract—Local variations in static slip, slip velocity, or rupture velocity contributes significantly to the information research on ground motions. Therefore, the characteristics of asperity and the position of the single asperity, are quantified to recognize its influence to the high-frequency radiation. In this paper a modified empirical Green's functions (EGF) method is suggested and used for ground motion simulation. The source parameters of asperity and rupture process are decided by the inhomogeneous fault. The synthesis of Tangshan earthquake in far field is used to study.

Keywords—software development, Tangshan earthquake, empirical Green's function, asperity, position

I. INTRODUCTION

Fifteen earthquakes were listed and analyzed by Somerville et al. [1]. All fifteen of these crustal earthquakes have rupture models in which the slip varies spatially over the fault surface. Many source and asperity parameters of these earthquakes were listed and analyzed by statistics. The asperity studied is defined to enclose fault elements whose slip is 1.5 or more times larger than the average slip over the fault and is subdivided if any row or column has an average slip less than 1.5 times the average slip [1]. The relation between the combined area of asperities S_a and seismic moment M_0 determined with constraining the slope to be 2/3 is:

$$S_a (km^2) = 5.00 \times 10^{-16} \times M_0^{2/3} (\text{dyne} \cdot \text{cm}) \quad (1.1)$$

Source modeling of recent shallow intraslab earthquakes was studied by using strong-motion data by Asano et al. [2]. They maintained that the ratio between the combined area of strong-motion generation areas and the area predicted by the empirical relationship tends to decrease with focal depth. The stress drops on strong motion generation areas (or asperities) of shallow intraslab earthquakes increase with focal depth.

A dynamic model of a single, isolated asperity was used as a simulation for a small aftershock of 1975 Oroville

earthquake by Das and Boatwright [3]. The acceleration waveforms and envelopes from a small aftershock were modeled by the failure of an asperity. By comparison, the continuing acceleration which follows the asperity failure process cannot be modeled exactly by using the method which assumes no further stress drop occurs during the equilibration of slip outside the asperity. The simpler problem of radiation from the fracturing of a circular asperity at the center of a circular fault was studied by Das and Kostrov [4]. Preliminary evidence suggests that the average stress drop on the asperity is increased by a certain ratio over the average stress drop that had previously occurred over the annular region of the fault. A static model for asperities were put forward by assuming that motion on the fault is resisted primarily by a patch of small strong asperities that interact with each other to increase the amount of displacement needed to cause failure by Johnson and Nadeau [5]. This asperity patch is surrounded by a much weaker fault that continually creeps in response to tectonic stress. They assumed that the moment release is triggered by the failure of the strong asperity patch and most of the moment comes from the displacement shadow. The assumption is that the stress drop on the none-asperity is zero when the asperities fail in this method. Were all of the asperities to rupture and the displacement deficit released, they get the scalar moment M_a of such an event would be

$$M_a = 4\mu D_a r_a R \quad (1.2)$$

Where r_a is the radius of the strong asperity patch, R is the outer radius of the displacement shadow, μ is the shear modulus.

An asperity was defined as a region in which the slip is larger by a prescribed amount than the average slip over the fault surface [5]. Based on the earthquakes researched by Somerville et al. [1], Wudi [6] get the average stress drops on all the asperities by statistics based on 15 earthquakes. The average stress drop on the asperities is

978-1-4244-5265-1/14/0826.00 ©2010 IEEE

II. THE INFLUENCE OF THE RELATIVE LOCATION OF THE ASPERITY ON THE FAULT ON THE FAR FIELD RESPONSE SPECTRUM

Firstly, the main shock fault plane is divided into asperity area and non-asperity area. The stress drop on the asperity is assumed to be the average stress proposed by equation (1.3). And the asperity area is divided into small cells. The non-asperity area also can be divided into small non-asperity cells.

A modified empirical Green's functions (EGF) method is suggested by Wudi [6], in which the asperity cells have the same stress. The record of small aftershock is needed to modify into that radiated from the small asperity cell and the small non-asperity cell. Each small cell will produce the wave when the propagating rupture reaches the cell. So that the ground motions of main shock can be synthesized by the waves radiated from the asperity cells and non-asperity cells as follows:

$$u(t) = \sum_{i=1}^{N_t} \sum_{j=1}^{N_n} u_{nij}(t - t_{nrj} - t_{ncij}) + \sum_{k=1}^{N_{at}} \sum_{m=1}^{N_{am}} u_{akm}(t - t_{arkm} - t_{ackm}) \quad (2.1)$$

Where, $t_{arkm} = |\xi_0 - \xi_{akm}| / V_r$ and $t_{ackm} = |R_s - R_{akm}| / V_c$ denote the time delay for the rupture propagation and the wave propagation of the (k, m) asperity cell, $t_{nrj} = |\xi_0 - \xi_{nrj}| / V_r$ and $t_{ncij} = |R_s - R_{nij}| / V_c$ denote the time delay for the rupture propagation and the wave propagation of the (i, j) non-asperity cell. ξ_0 , ξ_{akm} and ξ_{nrj} denote the coordinate of the rupture beginning location in main shock, the (k, m) asperity cell and the (i, j) none-asperity cell. V_r and V_c denote the velocity of rupture on the fault and wave propagation. R_s , R_{akm} and R_{nrj} denote the source distance of the aftershock, the distance from the (k, m) asperity cell to the receiver and from the (i, j) none-asperity cell to the receiver.

The Tangshan earthquake is considered as two sub-faults which consists of southern sub-faults striking N30°E and northern sub-faults strikes N50°E in the simulation [7] [8]. The main shock epicenter is located at the southern part. The sub-faults are shown in Table 1 in detail.

The seismic parameters of the main shock were determined by some reports mentioned above. The μ and the quality factor Q are considered as $3.3 \times 10^{10} N/m^2$ and 500, respectively.

The records of the Ninghe earthquake (MS = 6.9) are chosen as Green function to synthesize the far-field accelerations of the main shock. The parameters of the aftershock are shown in Table 2 in detail.

The Tangshan earthquake and the Ninghe earthquake were recorded at Guanting station. The epicentral distance of the main shock at Guanting station is 228 km, and the epicentral distance of the Ninghe earthquake at Guanting station is 216 km. For all the asperities, the relation between the asperity area A_a and the fault A is proposed by

Somerville et al. [1]. The approximately asperity area A_a is given by

$$A_a = 0.22 \times A \quad (2.2)$$

In order to show the influence of relative location of the single asperity, the 22 percent of the fault area of Tangshan earthquake is taken as the single asperity. Several main shock models with single asperity in different location are considered, and the different locations of asperities are shown in Figure1.

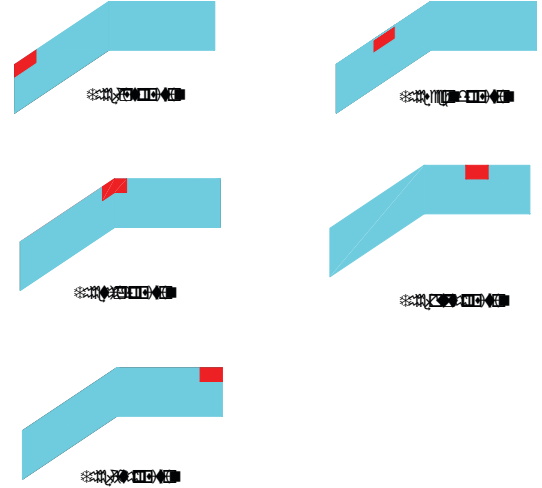


Figure 1. Five different locations on Tangshan earthquake fault

The rupture is assumed to start from right side of the fault, and rupture direction is from right to left. Figure 2 shows the response spectra (NW component) of the synthesized accelerations of the main shock at Guanting station. The response spectrum of observed Tanshan seismic acceleration is given out in Figure 2.

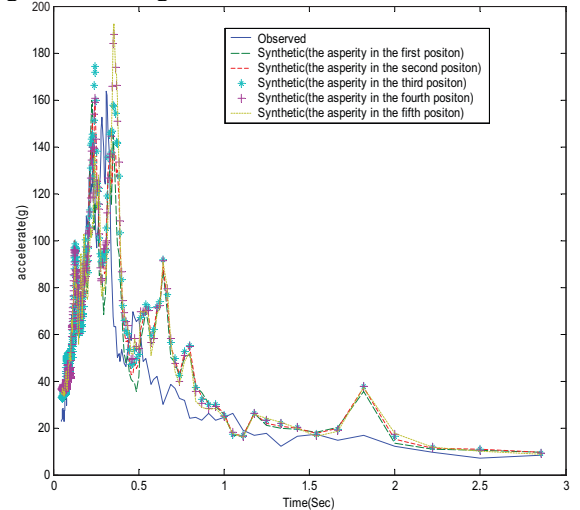


Figure 2. Comparison of response spectra of five synthesized accelerations with different asperity locations on the fault

Figure 2 shows that the synthetic response spectra have the same decay relationship in far field, and they are consistent with the response spectrum of observed record. It can be seen that the locations of asperity have large influence on response spectra in the period range from 0.2 to 0.4 second. The maximum values of response spectra decrease with the location which moving along the strike direction of the fault. And the peak value of response spectrum reaches the maximum when the single asperity is located at the rupture end of the fault. The locations of the asperities on the fault have less influence on response spectra in long period range.

III. CONCLUSIONS

The spectra of fault model with single asperity in different location on the fault have been simulated based on the empirical Green's functions method. Some conclusions could be reached from the simulated the Fourier amplitude spectrum of the single asperity.

The location of asperity has larger influence on response spectra in short period range than in long period range. The maximum values of response spectra decrease with the location which moving along the strike direction of the fault and the peak value reaches the maximum when the asperity locates at the rupture end of the fault.

IV. ACKNOWLEDGEMENTS

The research is supported by Supported by Research Fund for the Doctoral Program of Higher Education of China (20094410120002), Major Program of National Natural Science Foundation of China (90815027), the Open Foundation of Key Laboratory of Earthquake Engineering and Applied Technique of Guangdong Province and the Open Foundation of State Key Laboratory of Subtropical Building Science (2009KB17).

REFERENCES

- [1] Somerville P, Ikula K, Graves R, et al., "Characterizing crustal earthquake slip models for the prediction of strong ground motion", Seismological Research Letters, vol. 70, 1999, pp. 59-80.
- [2] Asano K, Iwata T and Irikura K., "Source characteristics of shallow intraslab earthquakes derived from strong-motion simulations". Earth Planets Space, vol. 55, 2003, pp. 5-8.
- [3] Das S and Boatwright J, "The breaking of a single asperity: Analysis of an aftershock of the 1975 Oroville, California, earthquake", Bull. Seim. Soc. Am. , vol. 75, 1985, pp. 677-687.
- [4] Das S and Kostrov B V, "Fracture of a single asperity on a finite fault: A model for weak earthquakes?" in Earthquake Source Mechanics, American Geophysical Union, Washington, D.C., 1986 pp.91-96.
- [5] Johnson L R and Nadeau R M, "Asperity model of an earthquake: static problem", Bull. Seim. Soc. Am. , vol. 92, 2002, pp. 672-686.
- [6] Wudi, "Synthesis and estimation of long period ground motions in far field and the characteristic of crustal seismic slip. Doctoral Dissertation, Tongji, published by Tongji University, Shanghai, pp.1-402
- [7] Zhou H L, "Some characteristics of source processes of large shallow strike-slip earthquakes", Acta Geophysica Sinica, vol.28, 1985, pp. 579-587 (in Chinese)
- [8] Luo Q F and Hu Y X, "Synthesis of accelerations of the 1976 Tangshan earthquake (MS 7.8) in near- and far-field by using semi-empirical method". Acta Seismologica Sinica, vol. 210, 1997, pp. 347-354.

TABLE I. THE SUB-FAULT PARAMETERS OF TANGSHAN EARTHQUAKE

Sub-fault	Strike $\phi(^{\circ})$	Dip $\delta(^{\circ})$	Rake $\lambda(^{\circ})$	M_0 ($\text{dyne} \cdot \text{cm}$)	$L \times W$ (km^2)	$\Delta\sigma$ (bar)	\bar{D} (cm)
1	30	80	180	7.1×10^{26}	57×20	20	186
2	50	80	180	6.9×10^{26}	57×20	19	186

TABLE II. THE PARAMETERS OF NINGHE EARTHQUAKE

Epicentre	Depth (km)	Strike	Dip	M_0 ($\text{dyne} \cdot \text{cm}$)	$L \times W$ (km^2)	$\Delta\sigma$ (bar)	\bar{D} (cm)
$39^{\circ}17'N$ $118^{\circ}47'E$	17	330°	39°	8.0×10^{25}	18×9	35	149.6